

CCA-1799

YU ISSN 0011-1643

UDC 543.42

Original Scientific Paper

In Situ Resonance Raman Spectroscopic Investigation of a Polypyrrole Modified Gold Electrode

H. R. Virdee and R. E. Hester*

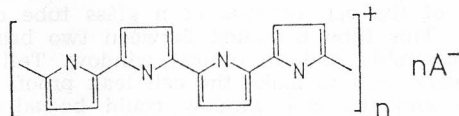
Department of Chemistry, University of York

Received December 7, 1987

Resonance Raman spectroscopy has been used *in situ* to study polypyrrole (PP) modified gold electrodes. Broad bands observed in the 1100—1600 cm^{-1} region of spectra of both oxidized (electrically conducting) PP^+ and the reduced insulating PP^0 forms have been interpreted in terms of the highly disordered structure of polypyrrole. Strong correlations between the band positions of polypyrrole and 2,5-dialkyl substituted pyrroles are noted and tentative assignments for polypyrrole bands are made from those of the 2,5-dialkyl pyrroles. The wavenumbers of bands at ca. 920—930, 1250—1260 and 1540—1550 cm^{-1} in the Raman spectra of polypyrrole show a strong correlation with bands observed in the Raman spectra of *cis*-polyacetylene. This suggests that the conjugated carbon chain backbones in polypyrrole and *cis*-polyacetylene are similar.

INTRODUCTION

Electrically conducting polypyrrole (PP) films, prepared by both chemical¹ and electrochemical²⁻⁸ oxidation of pyrrole, have attracted considerable attention in recent years, mainly because of their promise for application in devices such as modified electrodes for redox reactions⁹⁻¹¹, electrocatalysis⁸, and photocorrosion prevention in photoelectrochemical cells.¹²⁻¹⁹ Polypyrrole films can be formed from non-aqueous^{5-8,20} and aqueous²¹⁻²² media on a variety of electrode substrates. Chemical and physical properties^{20,23-28} suggest that the polymer is largely composed of linear chains of pyrrole rings joined by bands between the α -carbons so as to form an extended conjugated π -system. In its oxidized form, PP^+ , it is thought that approximately one pyrrole ring in three-to-four carries a positive charge.^{4-6,24,27} The polypyrrole chain may be represented as:



Anions, A^- , are incorporated into the polymer film to preserve overall charge neutrality. Polypyrrole in its conducting polycationic form, PP^+ , can be transformed into a neutral, PP^0 , insulating form by cathodic reduction. The

neutral PP° films are easily oxidized in air to give PP^+ . Cyclic voltammetry shows that, in the absence of oxygen, the film can be repeatedly cycled between the PP^+ and PP° forms.⁵

Elemental analyses^{5,29} of PP films indicate that the polymers are composed of about 66–75% by weight of pyrrole units and about 25–33% by weight of the counter anion from the electrolyte. Many different anions, both inorganic and organic, may be incorporated in PP^+ films. These include ClO_4^- , NO_3^- , BF_4^- , Cl^- , PF_6^- , SO_4^{2-} and toluene sulphonate. The physical properties, such as electrical conductivity³⁰ and electrochemical behaviour²⁰, of PP^+ films vary with the incorporated anions and also with the conditions of preparation and the solvent used.

The XPS,^{31,32} ^{13}C NMR³³ and IR^{28,37} spectroscopic evidence supports the view that intact pyrrole rings are present in these polymers. However, some structural disorder^{33,36} is evident from the XPS, ^{13}C NMR and x-ray diffraction studies⁷. Electron energy loss spectroscopic (EELS)³⁶ data have been interpreted in terms of a graphite-like structure with layers built from planar polymer chains.

Electronic absorption²⁸ spectra of PP show a strong broad absorption band at ca. 1.3 μm (1ev) and a much weaker band at ca. 400–500 nm (2–3 eV). The former absorption is thought to be associated with electron excitation into the conduction band⁷ of polypyrrole. The latter absorption arises from a localized $\pi-\pi^*$ transition of the pyrrole ring. In PP° spectra the band at ca. 400–500 nm is dominant. However, on exposure to O_2 the absorption spectrum of PP° becomes very similar to that of PP^+ , i.e. the 1.3 μm band dominates.

IR^{28,37} and Raman³⁷ spectra of detached PP films have been reported but no detailed analyses of those results have been carried out. Recently, *in situ* Raman spectra³⁸ of PP in its oxidized and reduced forms on indium tin oxide electrode in acetonitrile have been reported. Band assignments in the 1100–1700 cm^{-1} region have been made.

In this paper we report *in situ* resonance Raman spectroscopic (RRS) studies of electrochemically prepared PP^+ and PP° on gold electrodes in aqueous media, with various anions as counter ions. A rotating electrode was used in these experiments to prevent laser damage to polypyrrole films during Raman spectroscopic measurements.

EXPERIMENTAL

(a) Spectroelectrochemical Cell

The Raman spectroelectrochemical cell used in this work is shown in Figure 1. The design of the cell is based on a modification of that described by McQuillan and Hester. The body of the cell consists of a glass tube of 50 mm length and 2 mm wall thickness. This tube is bolted between two brass blocks which hold a rotating electrode assembly and an optical window. Teflon seals between the glass and the brass were used to make the cell leak proof. The distance between the electrode surface and the cell window could be adjusted by turning the rotating electrode bearing housing on its thread. A luggin capillary connected to the reference electrode was inserted through the neck of the electrochemical cell.

The working electrode was a gold disc, 7 mm in diameter and ca. 5 mm thick, moulded from 99.99% gold wire (Johnson-Matthey). This was attached to the

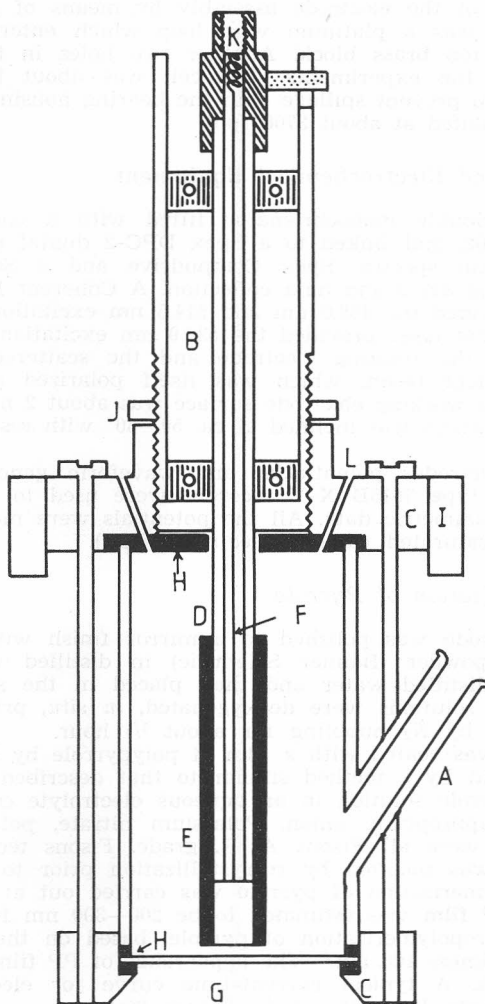


Figure 1. Raman spectroelectrochemical cell.

- A. Glas tube with a neck, for insertion of Luggin capillary.
- B. Rotating electrode bearing housing bolts.
- C. Brass blocks and clamping bolts.
- D. Rotating shaft.
- E. Teflon sleeve with Au electrode.
- F. Spring-loaded brass pin for making electrical contact.
- G. Quartz window.
- H. Teflon seals.
- I. Aluminium collar for clamping the cell in the sample housing of the Raman spectrometer.
- J. Locking nut.
- K. Brass slip ring together with carbon brush.
- L. Holes for entry for secondary electrode and for N_2 bubbles.

glass rotating shaft of the electrode assembly by means of a teflon sleeve. The secondary electrode was a platinum wire loop which entered the cell through a fine hole in the top brass block. Another two holes in this block facilitated N_2 -bubbling during the experiments. The cell was about half filled with the electrolyte solution to prevent spillage onto the bearing housing in all experiments the electrode was rotated at about 3700 rpm.

(b) Spectroscopic and Electrochemical Equipment

A Spex 1403 double monochromator fitted with a cooled photomultiplier, RCA type C31034-A02, and linked to a Spex DPC-2 digital photometer was used to record the Raman spectra. Spex Compudrive and a Scamp microcomputer controlled the grating drive and data collection. A Coherent Radiation Model CR4 argon ion laser provided the 488.0 nm and 514.5 nm excitation. A Spectra Physics Model 170 krypton ion laser provided the 530.9 nm excitation. The laser radiation was focused on to the rotating electrode and the scattered radiation collected at 90° to the incident beam, which was itself polarized perpendicular to the scattering plane. The working electrode surface was about 2 mm from and parallel to the cell window which was inclined at ca. 50 – 60° with respect to the vertically oriented laser beam.

An Oxford Electrodes potentiostat and waveform generator, together with a Hawlett Packard type 7015B X-Y recorder were used to control the potential and record the voltammetric data. All the potentials were measured and reported with respect to a saturated calomel electrode (SCE).

(c) Electropolymerization of Pyrrole

The gold electrode was polished to a mirror finish with a slurry of $1\ \mu\text{m}$ alumina polishing powder (Banner Scientific) in distilled water. The electrode was washed with distilled water and then placed in the spectroelectrochemical cell. All electrolyte solutions were deoxygenated, *in situ*, prior to electropolymerization of pyrrole, by N_2 bubbling for about $1/2$ hour.

The electrode was coated with a film of polypyrrole by electropolymerization. This was carried out by a method similar to that described by Pletcher et al.²¹, using a 50 mM pyrrole solution in an aqueous electrolyte containing 0.3 M concentration of the appropriate anion. Potassium nitrate, potassium sulphate and potassium chloride were all Fisons A. R. grade. Fisons technical grade sodium tetra fluoroborate was purified by recrystallization prior to use.

The electropolymerization of pyrrole was carried out at $+0.75\ \text{V}$ (SCE). The thickness of the PP film was estimated to be 200–300 nm from the current-time curve for the electropolymerization of pyrrole, based on the fact that $40\ \text{mC}/\text{cm}^2$ gives a coat of thickness 100 nm.⁴⁰ The appearance of PP films tended to be shiny dark blue to black. A typical current-time curve for electropolymerization of pyrrole on gold electrode is shown in Figure 2(a).

Cyclic voltammetric and Raman spectroscopic measurements were carried out in a pyrrole-free 0.1 M solution of an electrolyte containing the appropriate anion. A typical cyclic voltammogram from a polypyrrole film is shown in Figure 2(b).

The resonance Raman spectra (RRS) of PP^+ with NO_3^- , SO_4^{2-} , Cl^- and BF_4^- anions as counter ions were measured using 514.5 nm excitation. In each case the laser power used at the sample was less than 100 mW. The electrode was rotated at ca. 3700 rpm during all the Raman measurements.

RRS of PP^0 were recorded at $-0.05\ \text{V}$ (SCE) from solutions containing NO_3^- , SO_4^{2-} , Cl^- and BF_4^- anions, using 514.5 nm excitation.

RRS of PP^+ with NO_3^- as counter ion were also recorded using 488.0 nm and 530.9 nm excitations. RRS of PP with SO_4^{2-} as counter ion also were recorded at voltages ranging from $-0.25\ \text{V}$ to $0.45\ \text{V}$ (SCE) using 514.5 nm excitation.

Attempts to observe surface enhanced resonance Raman spectra (SERRS) were made by activating the gold electrode surface using a large number of oxidation reduction cycles (ORC's)⁴¹ on the gold electrode in 1 M KCl prior to the electropolymerization procedure. However, no significant increase in the Raman signal from polypyrrole films was observed in these experiments.

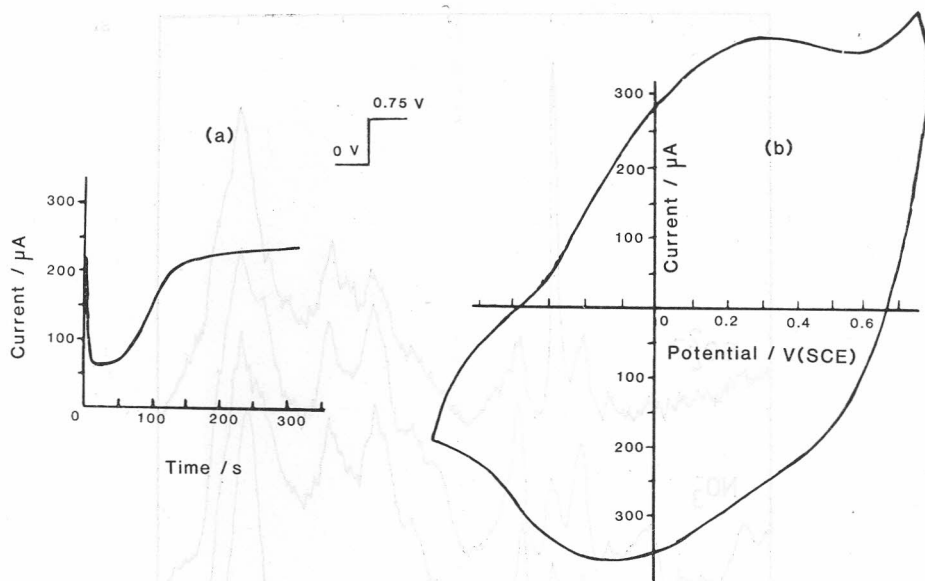


Figure 2. (a) Current-time curve for electropolymerization of pyrrole (50 mM) in 0.3 M aqueous KCl solution on gold electrode; (b) cyclic voltammogram of polypyrrole-modified gold electrode in 0.1 M KCl solution.

RESULTS

(a) RRS of Oxidized (PP^+) and Reduced (PP^\ominus) Polypyrrole

RRS of PP^+ doped with SO_4^{2-} , NO_3^- , Cl^- and BF_4^- counter ions are shown in Figure 3. The corresponding RRS of PP^\ominus are presented in Figure 4. These spectra are similar in general appearance to those reported for free-standing films³⁷ and on electrode surfaces.³⁸ The wavenumbers of the bands observed in the RRS of PP^\ominus and PP^+ with various counter anions are presented in Table I.

(i) Oxidized Polypyrrole, PP^+

As can be seen from Figure 3 and Table II, the RRS of PP^+ doped with SO_4^{2-} , NO_3^- , Cl^- and BF_4^- are dominated by very intense and broad features in the 1150–1600 cm^{-1} region. The most intense band is centred at ca. 1590 cm^{-1} in all cases except BF_4^- , where it appears at ca 1580 cm^{-1} . In each case the band is asymmetric in shape and there are shoulders both on the lower and higher wavenumber sides of the main peak. This suggests that the band is probably comprised of several overlapping bands.

A relatively strong band at ca 1410–1420 cm^{-1} and a broad feature centred at ca 1330 cm^{-1} are observed in all the spectra of PP^+ . Again this band appears to be comprised of a number of overlapping bands. A constant feature throughout this series of spectra is the appearance of a weak shoulder at ca. 1250–1260 cm^{-1} , irrespective of the counter ion present.

There are several quite clearly defined bands in the 550–1100 cm^{-1} region of this series of PP^+ spectra. The three most prominent ones are found

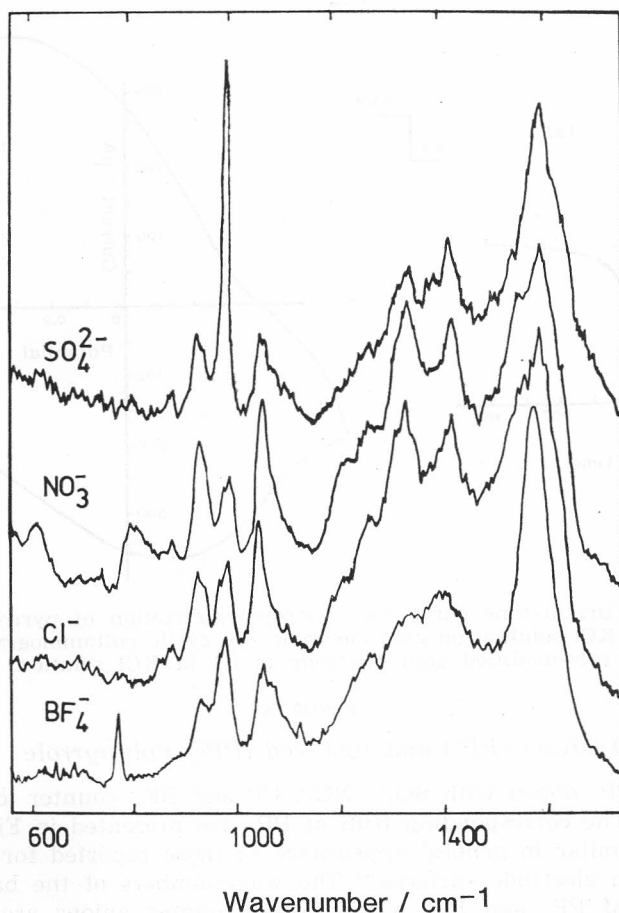


Figure 3. Resonance Raman spectra of PP^+ , with various counter anions, excited with 514.5 nm radiation.

at ca. 920–940, 980–995, and 1040–1050 cm^{-1} . The relatively large intensity of the 979 cm^{-1} band in the spectrum of PP^+ doped with SO_4^{2-} may be attributed to the fact that ν_1 vibration of SO_4^{2-} is contributing to the intensity of this band. Similarly there may be some contribution from the ν_1 of NO_3^- at ca. 1050 cm^{-1} in the spectrum of NO_3^- -doped PP^+ . However, there ca. 980–990 and 1050–1060 cm^{-1} in the spectra of Cl^- and BF_4^- -doped PP^+ , and at 1049 cm^{-1} in the spectra of nitrate-doped polypyrrole which can be attributed to polypyrrole itself. This is shown by the presence of bands at ca. 980–990 and 1050–1060 cm^{-1} in the spectra of Cl^- and BF_4^- -doped PP^+ .

A weak shoulder at ca 1070 cm^{-1} and a weak band at ca. 875 cm^{-1} are present in each of this series of PP^+ spectra, irrespective of the nature of the doping anion. In the case of nitrate-doped PP^+ two additional bands, at 792 and 605 cm^{-1} , appear. These bands are not apparent in the Raman spectra of PP^+ doped with the other anions. A sharp band at 768 cm^{-1} in the spectrum of BF_4^- -doped PP^+ can be attributed to the anion itself.

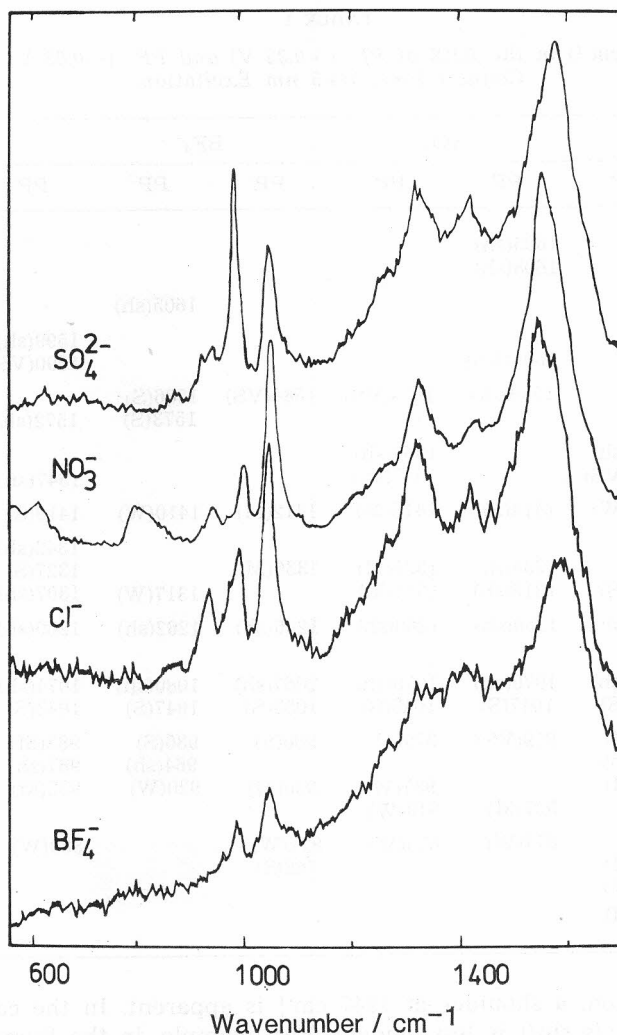


Figure 4. Resonance Raman spectra of PP^\ominus , with various anions in the supporting electrode, excited with 514.5 nm radiation.

(ii) *Reduced Polypyrrole, PP^\ominus*

Again, as in the case of PP^+ , the RR spectra of PP^\ominus (Figure 4) are dominated by broad features in the 1150–1600 cm^{-1} region. In general the bands appear to peak at a lower wavenumber than in the case of PP^+ . This shift is most clearly apparent in the spectra of PP^\ominus produced by electroreduction in the presence of NO_3^- and Cl^- ions. For example, in the case of PP^\ominus with NO_3^- ion, the peak in the spectrum is found at 1550 cm^{-1} . This appeared as a shoulder in the corresponding spectrum of PP^+ (c.f. Figures 3 and 4). Similarly, in the case of PP^\ominus with Cl^- ion, the peak in the RR spectrum is seen at 1542 cm^{-1} . In the corresponding spectrum of PP^+ with

TABLE I

Band Positions (cm^{-1}) in the RRS of PP^+ (+0.35 V) and PP^\ominus (-0.05 V) with Various Counter Ions. 514.5 nm Excitation.

NO_3^-		SO_4^{2-}		BF_4^-		Cl^-	
PP^+	PP^\ominus	PP^+	PP^\ominus	PP^+	PP^\ominus	PP^+	PP^\ominus
1629(sh)		1625(sh) 1608(sh)			1605(sh)		
1598(sh) 1590(VS)		1594(VS) 1580(sh)	1579(VS)	1584(VS)	1586(S) 1573(S)	1599(sh) 1590(VS)	1590(sh) 1572(sh)
1563(sh) 1550(sh)	1567(sh) 1550(VS)		1566(sh) 1547(sh)			1547(sh)	1542(VS)
1416(s)	1420(W)	1414(S)	1418(M)	1412(M)	1410(W)	1419(S)	1415(M)
1332(S) 1322(sh)	1316(S)	1334(S) 1315(sh)	1325(M) 1314(M)	1336(M)		1342(sh) 1327(S)	1341(sh) 1322(S)
	1260(sh)	1250(sh)	1260(sh)	1256(sh)	1262(sh)	1260(sh)	1254(sh)
1251(sh)							
1068(sh) 1049(S)	1075(sh) 1044(S)	1070(sh) 1047(S)	1070(sh) 1043(S)	1067(sh) 1053(S)	1030(sh) 1047(S)	1074(sh) 1043(S)	1070(sh) 1042(S)
986(M) 973(sh) 940(sh) 929(S)	992(M) 970(sh) 936(M)	979(VS)	979(S) 937(W) 919(W)	980(S) 930(M)	986(S) 964(sh) 920(W)	983(M) 967(sh) 932(M)	989(M) 971(sh) 934(M) 926(sh)
875(W) 792(W) 732(W) 605(M)	790(M) 730(W) 606(M)	874(W)	870(W)	877(W) 768(S)		880(W)	875(W)

Cl^- as counter ion, a shoulder at 1547 cm^{-1} is apparent. In the cases of SO_4^{2-} and BF_4^- ions, this shift is less evident. For example, in the Raman spectrum of PP^\ominus with SO_4^{2-} ion the peak is centred at 1579 cm^{-1} and a shoulder is apparent at ca. 1547 cm^{-1} . In the corresponding PP^+ Raman spectrum the peak is at 1594 cm^{-1} and a shoulder at 1580 cm^{-1} . Similarly, for the BF_4^- ion there are two equally intense peaks at 1586 and 1573 cm^{-1} for the PP^\ominus case, whereas only one peak, at 1584 cm^{-1} , is apparent in the PP^+ spectrum.

A band at ca. 1410 – 1420 cm^{-1} in the Raman spectra of PP^\ominus appears to decrease in intensity compared with the corresponding band in the PP^+ Raman spectra. For example, in the case of NO_3^- counter anion the PP^+ band at 1416 cm^{-1} is almost as intense as the feature found at 1332 cm^{-1} in the PP^+ spectrum. However, in the PP^\ominus spectrum this (1420 cm^{-1}) band is much weaker. This result is generally valid also for the other anions.

There are changes in the band around 1330 cm^{-1} between the Raman spectra of PP^+ and PP^\ominus . In general, the centre of the band shifts to lower

wavenumber. For example, in the case of polypyrrole with NO_3^- as counter ion, a strong band at 1316 cm^{-1} is observed in the PP^\ominus spectrum, whereas for the corresponding PP^+ spectrum the band appears at 1332 cm^{-1} with a shoulder at ca. 1322 cm^{-1} . For the case of SO_4^{2-} a strong band at 1334 and shoulder at ca. 1315 cm^{-1} in the PP^+ spectrum shifts down to a doublet of medium intensity at 1325 and 1314 cm^{-1} in the PP^\ominus spectrum. For the BF_4^- case a band at 1336 cm^{-1} , of medium intensity, is observed in the case of PP^+ . In the corresponding PP^\ominus spectrum, only a weak band at 1317 cm^{-1} is seen. For polypyrrole with chloride as counter ion, a strong band at 1327 cm^{-1} with shoulders at ca. 1342 and 1307 cm^{-1} in the PP^+ spectrum changes to a strong doublet at 1322 and 1317 cm^{-1} with a shoulder at ca. 1341 cm^{-1} .

The bands at $1040\text{--}1050\text{ cm}^{-1}$ in the PP^+ spectra appear to shift down by $4\text{--}6\text{ cm}^{-1}$ in going to PP^\ominus in each case except Cl^- . For example, in the NO_3^- case, this band appears at 1049 cm^{-1} in the PP^+ spectrum and at 1044 cm^{-1} in PP^\ominus . This band is relatively less intense in the PP^\ominus spectrum than it is in PP^+ , thus indicating decreasing contribution from the NO_3^- band. In the case of SO_4^{2-} , this band appears at 1043 cm^{-1} in the PP^\ominus spectrum, whereas it is seen at 1047 cm^{-1} in the PP^+ spectrum. For the case of BF_4^- the band shifts from 1053 cm^{-1} for PP^+ to 1047 cm^{-1} for PP^\ominus . For the Cl^- case, the shift is smaller, the band moving from 1043 to 1042 cm^{-1} .

The trend in the $980\text{--}990\text{ cm}^{-1}$ band appears to be a shift to higher wavenumber in going from PP^+ to PP^\ominus . This is the case for NO_3^- , Cl^- and BF_4^- . For example, in the case of NO_3^- counter anion, this band is found at 986 cm^{-1} in the PP^+ spectrum and at 992 cm^{-1} in PP^\ominus . Similarly the corresponding wavenumbers are 980 and 986 cm^{-1} for BF_4^- and 983 and 989 cm^{-1} for Cl^- . However, in the case of SO_4^{2-} no apparent shift in this band is observed in going from PP^+ to PP^\ominus . This is thought to be mainly because the interference from the ν_1 of SO_4^{2-} (from the electrolyte solution) is still present even in the PP^\ominus case.

(b) Effect of Applied Potential on the Raman Spectra

Raman spectra of polypyrrole, with SO_4^{2-} as the counter ion, at various applied potentials are presented in Figure 5. Table II gives band positions in the spectra at these applied potentials. The positions of the six major bands observed in the $900\text{--}1600\text{ cm}^{-1}$ region of the spectrum were plotted against applied potential. These plots are presented in Figure 6. As can be seen, only the bands at ca. 1330 cm^{-1} and $1600\text{--}1570\text{ cm}^{-1}$ show any significant change. For the bands at $1410\text{--}1420$, $1040\text{--}1050$, 980 and $920\text{--}930\text{ cm}^{-1}$ there are only random changes in the band positions with applied potentials of between -0.25 and $+0.45\text{ V}$ (SCE). However, for the bands at ca. 1330 cm^{-1} and $1570\text{--}1600\text{ cm}^{-1}$ a clear trend is apparent. There is a general shift in the band position to a lower wavenumber as the applied potential is decreased. For example, at a potential of $+0.45\text{ V}$ bands at 1340 and 1602 cm^{-1} are observed. These shift down to 1319 and 1570 cm^{-1} , respectively at a potential of -0.25 V (SCE). In general, there is a gradual decrease in the overall intensity of the Raman spectra on changing the applied potential from about $+0.15$ to -0.25 V .

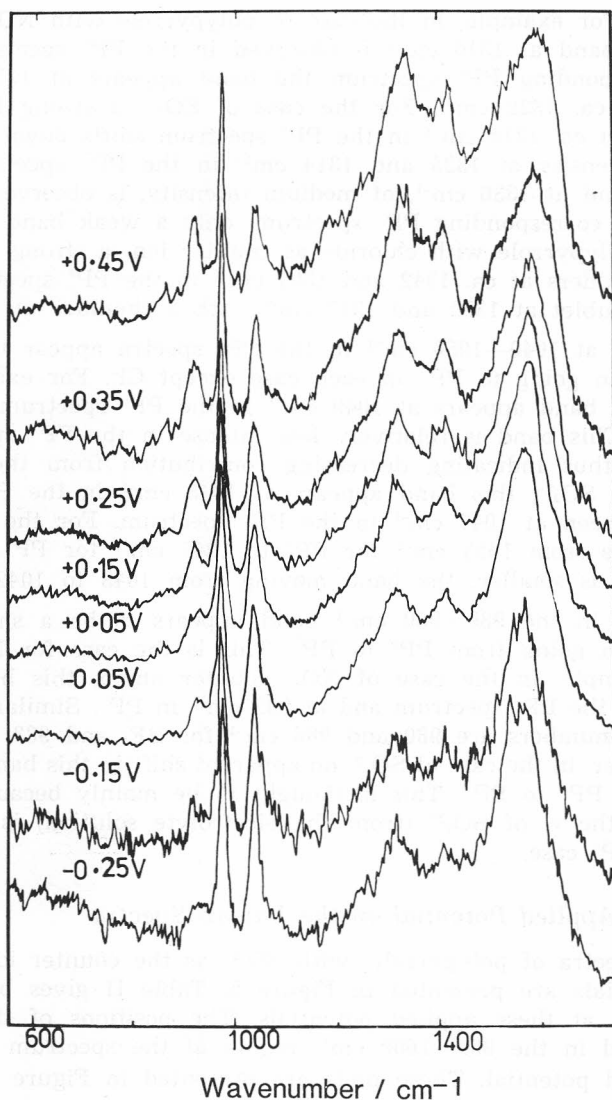


Figure 5. Resonance Raman spectra of polypyrrole, with SO_4^{2-} as counter ion, at various applied potentials (vs. SCE).

(c) *Excitation Wavelength-Dependence of the Raman Spectra of Polypyrrole*

Three different excitation wavelengths have been used in this work. Figure 7 shows the Raman spectra of NO_3^- -doped PP^+ excited with 488.0, 514.5 and 530.9 nm laser radiation. Also shown in Figure 7 are the Raman spectra of neutral polypyrrole excited at 488.0 and 514.5 nm. The positions of the bands observed in these spectra are given in Table III. A strong, broad band at 1599 cm^{-1} is observed in the 530.9 nm spectrum of PP^+ ,

TABLE II

Band Position (cm^{-1}) in the RRS of PP on Au Electrode, with SO_4^{2-} as Counter Ion, at Various Applied Potentials (vs. SCE). 514.5 nm Excitation.

-0.25 V	-0.15 V	-0.05 V	+0.15 V	+0.25 V	+0.35 V	+0.45 V
1606(sh)					1608(sh)	1625(sh) 1602(VS)
			1594(sh)	1590(VS)	1594(VS)	
1582(sh)	1586(sh)	1579(VS)	1583(VS)	1580(sh)	1580(sh)	
1573(VS)	1574(VS)	1566(sh)	1569(sh)	1563(sh)		
1554(sh)	1553(sh)	1547(sh)	1553(sh)	1540(sh)		1546(sh)
1413(W)	1418(M)	1418(M)	1415(M)	1415(M)	1414(S)	1415(M)
1320(M)	1319(S)	1325(S)	1325(S)	1330(S)	1334(S)	1340(S)
	1310(sh)	1314(S)	1310(sh)	1308(sh)	1315(sh)	
			1301(sh)			
1257(sh)	1261(sh)	1260(sh)	1260(sh)	1260(sh)	1250(sh)	1254(sh)
1057(sh)	1064(sh)	1070(sh)	1070(sh)	1069(sh)	1070(sh)	1063(sh)
1044(S)	1042(S)	1043(S)	1040(S)	1044(S)	1047(S)	1047(S)
979(VS)	979(VS)	979(VS)	978(VS)	979(VS)	979(VS)	979(VS)
925(W)	932(W)	928(W)	927(M)	927(M)	927(M)	928(M)
	875(W)	870(VW)	875(VW)	876(W)	874(M)	871(W)

whereas in that excited at 514.5 nm the strongest band is at 1590 cm^{-1} . There are shoulders on this band at ca. 1563, 1550 and 1537 cm^{-1} in the 530.9 nm spectrum. A strong band at 1320 cm^{-1} with a shoulder at ca. 1333 cm^{-1} is observed in the 530.9 nm spectrum. This is the reverse of the intensities observed in the 514.5 nm spectrum, where the band at 1332 cm^{-1} is the main peak with a shoulder at ca. 1322 cm^{-1} .

Another feature that is different in the Raman spectrum excited with 530.9 nm radiation is the clear resolution of the band at 1077 cm^{-1} . This band only appears as a very weak shoulder (at 1068 cm^{-1}) to the 1049 cm^{-1} band in the 514.5 nm spectrum. Bands at 792 cm^{-1} and 605 cm^{-1} , present in the Raman spectrum of $\text{PP}^+ \text{NO}_3^-$ excited with 514.5 nm radiation, are absent in the corresponding spectrum with 530.9 nm excitation.

A band at 1542 cm^{-1} in the Raman spectrum of NO_3^- -doped PP^+ excited with 488.0 nm radiation is clearly resolved and is the strongest feature in this spectrum. This band appears only as a shoulder to the strong bands at 1590 cm^{-1} and 1599 cm^{-1} in the corresponding Raman spectra excited with 514.5 and 530.9 nm radiation, respectively. Three other bands of slightly lower intensity, at 1592, 1584 and 1567 cm^{-1} , can be distinguished in the PP^+ spectra excited with 488.0 nm radiation. The other main differences are in the relative intensities of the bands at 980–990 cm^{-1} and 930–940 cm^{-1} .

In the case of 488.0 nm spectra the band at 980–990 cm^{-1} is stronger than that at 930–940 cm^{-1} . This is the reverse of what is found in the case of 514.5 nm and 530.9 nm spectra. The bands at ca. 800 and 600 cm^{-1} also are much stronger in the Raman spectra excited with 488.0 nm radiation.

In the spectra of PP^\ominus excited with 488.0 nm radiation the band at 1542 cm^{-1} is dominant (See Figure 7(b)), the band at ca. 1584 cm^{-1} appearing as

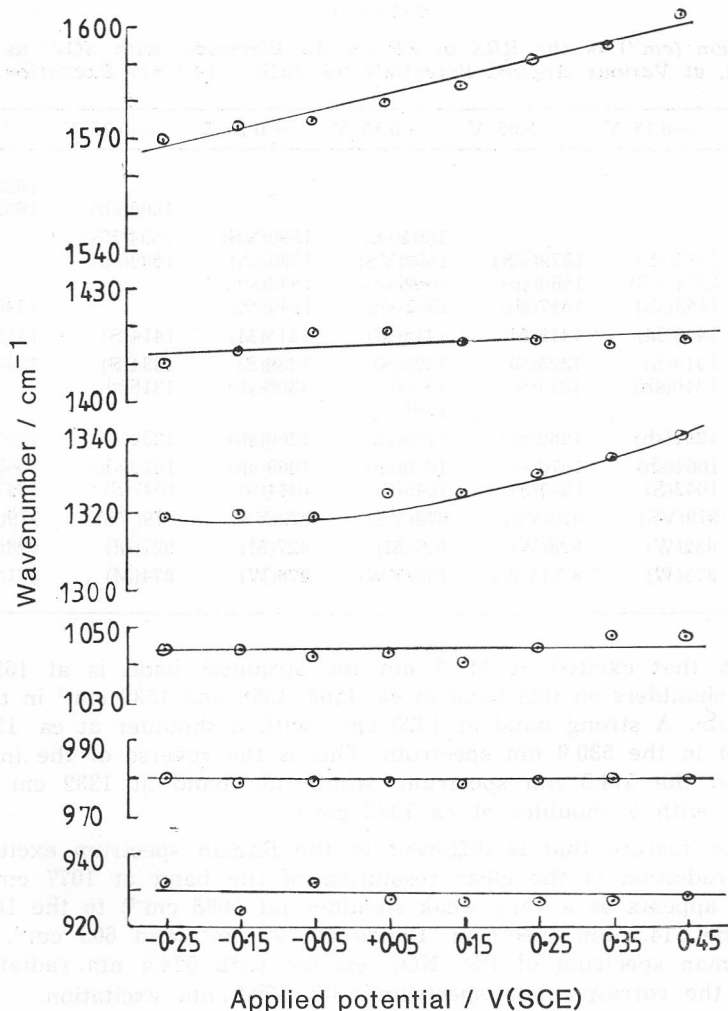


Figure 6. Variation of band positions with applied potential, of PP^+ on Au electrode, with SO_4^{2-} as counter ion.

a shoulder. The remainder of the Raman spectrum appears to be very similar to that given by PP^+ . However, more striking differences are apparent between the PP° and PP^+ spectra excited at 514.5 nm, as is immediately seen from Figure 7(a).

DISCUSSION

The broad bands centred at 1320–1340 cm^{-1} and 1570–1600 cm^{-1} in the RRS of various samples of polypyrrole resemble closely those observed from various types of graphitic carbon. The appearance of graphitic carbon bands in the Raman spectra from silver electrode surfaces has been investigated by Cooney *et al.*^{49,43} who observed two bands at 1580 + 10 and

$1360 + 20 \text{ cm}^{-1}$. The relative intensities of these bands changed with the applied potential and they disappeared at very negative potentials (-1.2 V , SCE), when the graphitic carbon present on the electrode surface is thought to be reduced to hydrocarbons which then desorb from the electrode surface. More recently, McQuillan and Hester³⁹ have reported Raman spectra from different types of pyrolytic graphite electrodes in acidic media under various potential conditions. A sharp band at 1580 cm^{-1} and two very weak features at 1618 and 1330 cm^{-1} were observed when the graphite electrode was held at 0 V (SCE). On changing the potential of the electrode to $+1.8$

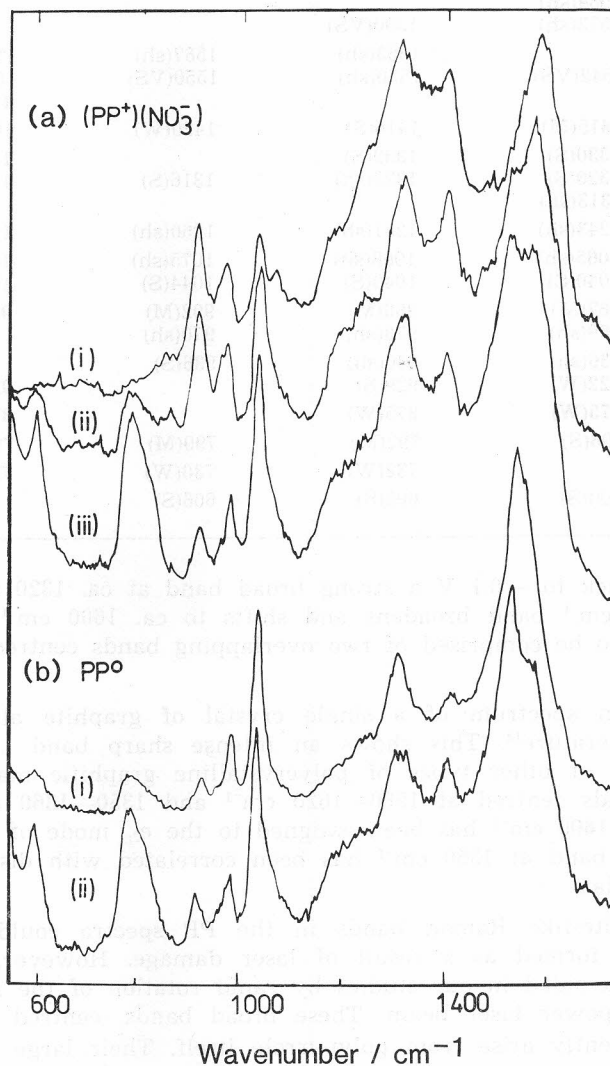


Figure 7. Resonance Raman spectra of (a) PP^+ with NO_3^- as counter ion, excited with 530.9, 514.5, and 488.0 nm radiation; (b) PP^0 excited with 514.5 and 488.0 nm radiation.

TABLE III

Band Position (cm^{-1}) of RRS of PP on Au Electrode Excited with 514.5, 488.0 and 530.9 nm Laser Radiation

488.8 nm		514.5 nm		530.9 nm
(PP ⁺) (NO ₃ ⁻)	PP ^o	(PP ⁺) (NO ₃ ⁻)	PP ^o	(PP ⁺) (NO ₃ ⁻)
		1629(sh)		
1592(sh)		1598(sh)		1599(VS)
1584(sh)	1584(sh)			
	1573(sh)	1590(VS)		
1567(sh)		1563(sh)	1567(sh)	1563(sh)
1542(VS)	1542(VS)	1550(sh)	1550(VS)	1550(sh)
				1537(sh)
1416(M)	1415(M)	1416(S)	1420(W)	1414(S)
1332(S)	1330(S)	1332(S)		1333(sh)
1321(sh)	1320(S)	1322(sh)	1316(S)	1320(S)
1305(sh)	1313(sh)			
1255(sh)	1243(sh)	1251(sh)	1260(sh)	1257(sh)
1060(sh)	1065(sh)	1068(sh)	1075(sh)	1077(M)
1044(S)	1040(S)	1049(S)	1044(S)	1044(S)
990(M)	987(M)	986(M)	992(M)	980(S)
971(sh)	969(sh)	973(sh)	970(sh)	
	936(sh)	940(sh)	936(S)	
929(W)	922(W)	929(S)		924(S)
875(W)	875(W)	875(W)		875(W)
798(S)	796(S)	792(M)	790(M)	793(W)
732(W)		732(W)	730(W)	726(W)
602(S)	600(S)	605(S)	606(S)	

V and then back to -0.1 V a strong broad band at ca. 1320 cm^{-1} appears and the 1580 cm^{-1} band broadens and shifts to ca. 1600 cm^{-1} . This latter band appears to be comprised of two overlapping bands centred at ca. 1595 and 1608 cm^{-1} .

The Raman spectrum of a single crystal of graphite also has been reported in literature⁴⁴. This shows an intense sharp band at 1575 cm^{-1} . Raman spectra of other types of polycrystalline graphitic materials show two broad bands centred at $1580\text{--}1620\text{ cm}^{-1}$ and $1350\text{--}1360\text{ cm}^{-1}$.^{44,45} The band at $1580\text{--}1600\text{ cm}^{-1}$ has been assigned to the e_{2g} mode of the graphite structure. The band at 1350 cm^{-1} has been correlated with disorder in the graphite materials.

The graphite-like Raman bands in the PP spectra could arise from carbon species formed as a result of laser damage. However, we believe that this was avoided in our studies by rapid rotation of the samples in a relatively low-power laser beam. These broad bands, centred at 1590 and 1330 cm^{-1} evidently arise from polypyrrole itself. Their large band widths suggests a disordered structure. This supports the interpretation of EELS data³⁶ for polypyrrole in which the polypyrrole itself is thought to have graphite-like structure, with the layers built up from planar polymer chains,

with dopant anions occupying spaces between the chains within the layers rather than intercalating between the basal planes.

Tentative assignments of the other bands observed in the RRS of polypyrrole have been made by comparing their wavenumbers and intensities in the spectra of pyrrole and 2,5-dialkyl substituted pyrroles, as reported in literature.^{46,47} The band positions of pyrrole, 2,5-dialkyl pyrrole, and polypyrrole, together with some tentative assignments, are listed in Table IV.

TABLE IV

Band Positions (cm⁻¹) in the RRS of PP⁺ and PP⁰ Compared with Those Observed for Pyrrole and 2,5-dialkyl Pyrroles, Together with some Tentative Assignments

Pyrrole ^a	2,5-dialkyl ^a pyrroles	PP ⁺ ^b	PP ⁰ ^b	Assignments
1467	1605	1590		ν (C=C)
	1514	—	1550	
1379	1418	1416	1420	ν CN
		1332	1316	
	1258	1251	1260	ring breathing
1142				
1076		1068	1075	δ (CH)
1045	1034	1049	1044	
	999	986	992	γ (CH)
		929	936	
866		875		
839	765	792	790	δ (ring)
735		732	730	
711				γ (ring)
644				
	603	605	606	

^a Ref 45

^b present work 514.5 nm excitation, NO₃⁻ anion

ν = stretching vibration

δ = in-plane deformation

γ = out-of-plane deformation

The strongest band in the Raman spectrum of pyrrole itself is observed at 1142 cm⁻¹ and has been assigned⁴⁶ to the »ring-breathing« mode of the pyrrole molecule. As can be seen from Table IV, this band does not appear in the Raman spectra of 2,5-dialkyl pyrroles. Similarly, this band is absent in the Raman spectrum of polypyrrole. A band at 1467 cm⁻¹ in the pyrrole spectrum, assigned to the C=C symmetric stretching vibration, shifts to 1514 cm⁻¹ in the spectra of 2,5-dialkyl pyrroles. In the spectrum of PP⁰ the bands at ca. 1550 cm⁻¹ are tentatively assigned to C=C stretching vibrations.

A band at 1418 cm⁻¹ in the Raman spectra of 2,5-dialkyl pyrroles, thought to be due to the C—N stretching vibration, correlates well with one at ca. 1420 cm⁻¹ in the polypyrrole spectra. There also is a very good correlation between the band reported at 1258 cm⁻¹ for 2,5-dialkyl pyrroles and one which appears as a shoulder on the graphite-like band centred at ca. 1320 cm⁻¹ throughout the series of spectra reported here, i. e. at 1250—1260 cm⁻¹ in the polypyrrole spectra. Two bands, at 1076 and 1045 cm⁻¹, assigned to the CH in-plane deformation in pyrrole, can be correlated with the bands

at 1060—1080 cm^{-1} and at 1040—1050 cm^{-1} in the polypyrrole spectra. There is a similar agreement between the band position at 999 cm^{-1} in 2,5-dialkyl pyrroles and at 986—992 cm^{-1} in polypyrrole. A band at 875 cm^{-1} in the PP^+ spectrum is tentatively assigned to the out-of-plane C—H deformation, by comparison with one at 866 cm^{-1} in the spectrum of pyrrole. A weak band at 730—735 cm^{-1} in the spectrum of PP^+ has its counterpart in the pyrrole spectrum at 735 cm^{-1} , where it has been assigned to an out-of-plane CH deformation. A band at 603 cm^{-1} in the spectra of 2,5-dialkyl pyrroles has been assigned to an out-of-plane deformation of the pyrrole ring, corresponding to the 605 cm^{-1} band in the polypyrrole spectra.

Polypyrrole is believed to have an extended conjugated π -electron system.^{29,48} The RRS of PP accordingly may be expected to show some correlation with that of polyacetylene^{49,50}, which is also a conjugated polymer and an electrical conductor. In *trans*-polyacetylene the wavenumber of the conjugated C=C stretching vibration is observed in the 1460—1600 cm^{-1} range, depending on the wavelength of the excitation of the RR spectra. For example, with red excitation at 676.4 nm the conjugated C=C stretching band is observed at 1466 cm^{-1} . This band shifts to 1485 cm^{-1} when the spectrum is excited with 514.5 nm radiation. Excitation with 325.0 nm radiation shifts the band to 1596 cm^{-1} . This appearance of the C=C stretching mode at various wave-lengths leads to a band at 1477 cm^{-1} ,⁴⁹ which has been attributed to an all-*trans* segment in polyacetylene.^{49,50} Thus the band at 1466 cm^{-1} in the 676.4 nm RR spectrum of polyacetylene has been assigned to an all-*trans* segment of 100 conjugated C=C bonds. Similarly, excitation with 530.9 nm radiation gives rise to a band at 1477 cm^{-1} ,⁴⁹ which has been attributed to an all-*trans* segment of ca. 30 conjugated C=C bonds. A band at 1485 cm^{-1} ⁴⁹ observed with 514.5 nm excitation corresponds to an all-*trans* segment of about 25 conjugated C=C bonds, and the 1496 cm^{-1} ⁴⁹ band, observed with 488.0 nm excitation, corresponds to an all-*trans* segment length of 17—20 conjugated C=C bonds.

In the RR spectra of PP there is a similar, though lesser, dependence on the wavelength of the excitation radiation. However, the wavenumber of the C=C stretching mode in PP has the opposite dependence on excitation wavelength from that observed for all-*trans* polyacetylene. For the three wavelengths used to excite the RR spectra of PP^+ , namely 488.0, 514.5, and 530.9 nm, the C=C stretching mode is observed at 1542, 1590, and 1599 cm^{-1} , respectively (see Table III). However, if a comparison of the PP spectra is made with the RR spectra of *cis*-polyacetylene, there is seen to be a strong correlation between the wavenumbers of the RR bands. In the *cis*-polyacetylene spectrum three strong bands at 920, 1250—1260 and 1540—1550 cm^{-1} ⁴⁹ are observed with excitation in the 647 to 350 nm range. As can be seen from Table 3, corresponding bands also are present in the RR spectra of PP. Within the individual pyrrole rings the conjugated double bonds are, of course, intrinsically locked into the *cis*-geometry. However, both *cis* and *trans* arrangements are possible for adjacent rings. Although it is not obvious that the inverse wavelength/wavenumber correlation noted for PP as compared with polyacetylene would be expected on the basis of their respective structures, we tentatively conclude that our results may be interpreted in terms of *trans* segments of variable length interspersed with all-*cis* bends in the

otherwise linear polymer chains. Unlike polyacetylene, the *trans* segments of PP incorporate intrinsically an alternating *cis/trans* configuration of C=C bonds which evidently leads to the observed behaviour. The 10–15 cm⁻¹ increase in wavenumber of the ν (C=C) mode in going from PP⁰ to PP⁺ (see Table I) is unexpected in suggesting increased C=C bond order in PP⁺. Probably this is a result of decreased lone-pair electron correlation in PP⁺.

Acknowledgements. — We are grateful to the SERC for financial support of this work.

REFERENCES

1. M. Salmon, K. K. Kanazawa, A. F. Diaz, and M. Krounbi, *J. Polym. Sci. Polymer Lett., Ed.*, **20** (1982) 187.
2. A. F. Diaz, K. K. Kanazawa, and G. P. Gardini, *J. Chem. Soc. Chem. Commun.* 1979, 635.
3. K. K. Kanazawa, A. F. Diaz, R. H. Geiss, W. D. Gill, J. F. Kwak, J. A. Logan, and J. F. Rabolt, *J. Chem. Soc. Chem. Commun.* 1979, 854.
4. A. F. Diaz and J. I. Castillo, *J. Chem. Soc. Chem. Commun.* 1980, 397.
5. A. F. Diaz, *Chem. Scr.* **17** (1981) 145.
6. P. Burgmayer and R. W. Murray, *J. Electroanal. Chem. Interfacial Electrochem.* **104** (1982) 6139.
7. G. B. Street, T. C. Clarke, K. K. Krounbi, P. Pfluger, J. F. Rabolt, and R. H. Geiss, *Polym. Prepr.* **23** (1982) 117.
8. R. A. Bull, F. R. Fan, and A. J. Bard, *J. Electrochem. Soc.* **130** (1983) 1636.
9. K. S. V. Santhanam and R. N. O'Brien, *J. Electroanal. Chem. Interfacial Electrochem.* **160** (1984) 377.
10. A. F. Diaz, J. J. Crowley, J. Bargon, G. P. Gardini, and J. B. Torrence, *J. Electroanal. Chem. Interfacial Electrochem.* **121** (1981) 355.
11. R. A. Bull, F. R. Fan, and A. J. Bard, *J. Electrochem. Soc.* **129** (1982) 1009.
12. R. Noufi, D. Tench, and L. F. Warren, *J. Electrochem. Soc.* **127** (1980) 2310.
13. R. Noufi, D. Tench, and L. F. Warren, *J. Electrochem. Soc.* **128** (1981) 2596.
14. R. Noufi, A. J. Frank, and A. J. Nozik, *J. Electroanal. Chem. Interfacial Electrochem.* **103** (1981) 1849.
15. T. Skotheim, I. Lundstrom, and J. Prejza, *J. Electrochem. Soc.* **128** (1981) 1625.
16. F. R. Fan, B. Wheeler, A. J. Bard, and R. Noufi, *J. Electrochem. Soc.* **128** (1981) 2042.
17. R. A. Simon, A. J. Ricco, and M. S. Wrighton, *J. Am. Chem. Soc.* **104** (1982) 2431.
18. A. J. Frank and R. J. Honda, *J. Phys. Chem.* **86** (1982) 1933.
19. A. J. Frank, *Mol. Cryst. Liq. Cryst.* **83** (1982) 341.
20. A. F. Diaz and B. Hall, *IBM J. Res. Dev.* **27** (1983) 342.
21. S. Asavapiriyant, G. R. Chandler, G. A. Gunawardena, and D. Pletcher, *J. Electroanal. Chem. Interfacial Electrochem.* **177** (1984) 229.
22. G. Mengoli, M. M. Musianni, M. Fleischmann, and D. Pletcher, *J. Appl. Electrochem.* **14** (1984) 285.
23. W. R. Selaneck, R. Erlandsson, J. Preijza, I. Lundstrom, and O. Inganas, *Synth. Met.* **5** (1983) 125.
24. W. K. Ford, C. B. Duke, and W. R. Selaneck, *J. Chem. Phys.* **77** (1981) 5031.
25. A. F. Diaz, J. I. Castillo, J. A. Logan, and W. Y. Lee, *J. Electroanal. Chem. Interfacial Electrochem.* **129** (1981) 115.
26. E. M. Genies, G. Bidan, and A. F. Diaz, *J. Electroanal. Chem. Interfacial Electrochem.* **149** (1983) 101.
27. O. Inganas, T. Skotheim, and I. Lundstrom, *J. Appl. Phys.* **54** (1983) 3636.

28. P. Pfluger, M. Krounbi, G. B. Street, and G. Weiser, *J. Chem. Phys.* **78** (1983) 3212.
29. M. Salmon, A. F. Diaz, A. J. Logan, M. Krounbi, and J. Bargon, *Mol. Cryst. Liq. Cryst.* **83** (1983) 265.
30. A. F. Diaz, J. M. Vasquez Vallejo, and A. Martinez Durran, *IBM, J. Res. Dev.* **25** (1981) 42.
31. P. Pfluger and G. B. Street, *JK. Chem. Phys.* **80** (1984) 544.
32. W. R. Salaneck, R. Erlandsson, J. Prezja, I. Lundstrom, C. B. Duke, and W. K. Ford, *Polymer Prepr.* **23** (1982) 120.
33. J. C. Scott, P. Pfluger, T. C. Clarke, and G. B. Street, *Polymer Prepr.* **23** (1982) 119.
34. A. Nazzari and G. B. Street, *J. Chem. Soc. Chem. Commun.* 1984, 83.
35. W. Wernet, M. Monkenbusch, and G. Wegner, *Mol. Cryst. Liq. Cryst.* **118** (1985) 193.
36. J. Fink, B. S. Scheerer, W. Wernet, M. Monkenbusch, G. Wegner, H. J. Freund, and H. Gonska, *Phys. Rev.* **34** (1986) 1101.
37. L. Oddi, R. Capaletti, R. Fieshi, M. P. Fountana, V. Bocchi, and G. P. Gardini, *Mol. Cryst. Liq. Cryst.* **118** (1985) 179.
38. T. Inoue, I. Hosoya, and T. Yamase, *Chem. Lett.*, 1987, 563.
39. A. U. McQuillan and R. E. Hester, *J. Raman Spectroscopy* **15** (1984) 15.
40. J. E. Prezeworskii, *Ph. D. thesis*, Imperial College, University of London, 1984.
41. P. Gao, M. L. Patterson, M. A. Taddyoni, and M. J. Weaver, *Langmuir* **1** (1985) 173.
42. M. R. Mahoney, M. N. Howard, and R. P. Cooney, *Chem. Phys. Lett.* **71** (1980) 59.
43. M. N. Howard, R. P. Cooney, and A. J. McQuillan, *J. Raman Spectroscopy* **9** (1980) 273.
44. F. Tuinstra and J. L. Koenig, *J. Chem. Phys.* **53** (1970) 1126.
45. C. A. Johnson and K. M. Thomas, *Fuel* **63** (1984) 1073.
46. F. R. Dollish, W. G. Fateley, and F. F. Bentley, *Characteristic Raman Frequencies of Organic Compounds*, John Wiley and Sons, New York, 1974.
47. D. W. Scott, *J. Mol. Spectrosc.* **37** (1971) 77.
48. K. Yakushi, L. J. Lauchlan, T. C. Clarke, and G. B. Street, *J. Chem. Phys.* **79** (1983) 4774.
49. D. N. Batchelder and D. Bloor in *Advances in Infrared and Raman Spectroscopy* Vol. **11** (R. J. H. Clark and R. E. Hester, eds.), Wiley, Chichester, 1984, p. 190.
50. I. Harada, M. Tasumi, H. Shirakawa, and S. Ikeda, *Chem. Lett.* 1978, 1411.

SAŽETAK

Istraživanje *in situ* rezonantnih Ramanovih spektara zlatne elektrode modificirane polipirolom

H. R. Virdee i R. E. Hester

Rezonantna Ramanova spektroskopija primijenjena je *in situ* na studij zlatne elektrode modificirane polipirolom (PP). Široke vrpce, zapažene u području 1100–1600 cm^{-1} u spektrima i oksidiranog (električki vodljivog) PP^+ i reduciranog izolirajućeg PP^0 oblika, interpretirane su u smislu visokog nereda u strukturi polipirola. Zapažena je jaka korelacija između položaja vrpce polipirola i 2,5-dialkil-supstituiranih pirola, te provedena provizorna asignacija za vrpce polipirola prema onima 2,5-dialkilpirola. Valni brojevi vrpce na oko 920–930, 1250–1260 i 1540–1550 cm^{-1} u Ramanovim spektrima polipirola pokazuju jaku korelaciju s vrpčama opaženim u Ramanovim spektrima *cis*-poliacetilena. To upućuje na sličnost konjugiranih lanaca ugljika u polipirolu i *cis*-poliacetilenu.